Robust Ultrasensitive Transcriptional Switch in Noisy Cellular Environments

Authors

Eui Min Jeong[1,2], and Jae Kyoung Kim[1,2,*]

[1]Biomedical Mathematics Group, Institute for Basic Science, Daejeon 34126, Republic of Korea

[2]Department of Mathematical Sciences, Korea Advanced Institute of Science and Technology, Daejeon 34141, Republic of Korea

[*]Correspondence: jaekkim@kaist.ac.kr

Abstract

Ultrasensitive transcriptional switches enable cells to make sharp transitions between on and off states of transcription, essential for cells to respond to environmental cues with high fidelity. However, conventional switches that rely on direct repressor-DNA binding are extremely sensitive to noise, leading to unintended changes in gene expression. This raises doubts about the effectiveness of these switches in noisy cellular environments. Here, we find an alternative avenue, where the combination of different indirect transcriptional regulations generates a noise-resilient ultrasensitive switch. Specifically, when a transcriptional repressor inhibits a transcriptional activator through the combination of sequestration, blocking, and displacement instead of directly binding to DNA, a robust ultrasensitive switch is achieved. Sequestration alone can generate an ultrasensitive transcriptional response, but the switch remains vulnerable to noise because the undesired on or off state induced by noise can persist for a long period. However, by jointly utilizing blocking and displacement, noise-induced transitions can be rapidly restored to the original desired state. This transcriptional switch is effective in noisy cellular contexts, which makes it suitable for robust synthetic system design. Our findings also provide insights into the evolution of ultrasensitive switches in real cells. The concurrent use of seemingly redundant multiple indirect transcriptional repression mechanisms in diverse biological systems appears to be a strategy to improve the noise-resilience of ultrasensitive switches.

1. Introduction

Ultrasensitive responses are input/output relationships within biological systems, exhibiting a highly sensitive response to changes in input or stimulus [1]. In particular, transcriptional ultrasensitive switches are turned on or off depending on whether the number of the transcriptional factor exceeds or falls below a threshold. This distinctive property renders these switches valuable for systems requiring precise decision-making contingent on the number of input transcriptional factors. Moreover, these switches serve as catalysts for diverse cellular functions, including signal amplification and generation of bistability and oscillations [2, 3], thereby bestowing them with versatile utility across various biological contexts. The ultrasensitive transcriptional switch can be generated by the cooperative binding of transcriptional factors to multiple DNA binding sites [2, 3] or their titration via decoy sites [4]. However, recent studies have raised doubts about the effectiveness of these conventional transcriptional switches in noisy cellular environments [5, 6]. Specifically, when noise induces transitions between the transcriptional 'on' and 'off' irrespective of the number of the transcriptional factor, this undesired transition persists for a long time in these switches.

Alternatively, transcriptional repressors can suppress transcription indirectly by targeting transcriptional activator rather than directly binding to DNA [7, 8]. Specifically, repressors can sequester transcriptional activators, preventing their binding to DNA. For example, sigma factors or basic leucine zippers can be sequestered through interactions with anti-sigma factors or inhibitors, respectively [9-11]. Also, repressors can bind with activators already bound to DNA, leading to transcriptional inhibition. This blocking is utilized when PHO80, a kinase component in a signaling pathway of yeast, inhibits PHO4 [12]. In addition to sequestration and blocking, repressors can displace DNA-bound activators. An illustrative case is the IκB protein, which reduces NF-κB activator's binding affinity with DNA, displacing it from the DNA [13]. We recently found that the combination of the sequestration, blocking and displacement can generate ultrasensitive transcriptional switch [14]. Interestingly, these three indirect repression mechanisms synergistically function in systems like the NF-κB oscillator and circadian clocks [13, 15-19], where precise ultrasensitivity against noise is crucial. This implies that the ultrasensitive switch based on the combination of multiple indirect repression mechanisms could be robust against noise unlike the conventional switches relying on direct repression.

We found that the ultrasensitive switch based on the combination of the sequestration, blocking, and displacement can stably sustain the transcriptional ‘on’ and ‘off’ states even in the presence of noise. Specifically, our research has unveiled that the combined integration of these three repression mechanisms immediately restores the original 'off' and 'on' states even when noise triggers transitions to the undesired transcriptional states. In this switch, the sequestration generates a sharp transition from the transcriptional ‘on’ state to the ‘off’ state as the molar ratio between repressors and activators shifts from below one to above one. Furthermore, even if the transcriptional ‘off’ state transits to the ‘on’ state due to noise, the blocking rapidly restores the original ‘off’ state when the molar ratio surpasses one. In addition, the displacement ensures that the noise-induced transcriptional ‘on’ state swiftly returns to the original ‘off’ state when the molar ratio falls below one. Taken together, we propose an ultrasensitive transcriptional switch that can operate effectively even in noisy cellular environments and can offer promising strategy for designing robust synthetic switches.

2. Results

2.1. Noise triggers both activation during TRP and repression during TAP of the cooperative binding-based switch.

Ultrasensitivity can be generated through the cooperative binding of transcriptional repressors to multiple DNA sites [3, 20]. To investigate this mechanism, we used a previously developed model [5] (Fig. 1A). In the model, the DNA has three sites that can bind with the repressor (R) with a dissociation constant of K_r. When one site of the DNA is occupied, R can bind to the other two sites with a dissociation constant of cK_r. Similarly, when two sites of the DNA are occupied, then R can bind to the remaining site with a dissociation constant of c^2K_r. Therefore, in the case where $c = 1$, R binds independently to three sites, but in the case where $c < 1$, R more favorably binds to the DNA where one site or two sites is occupied than the DNA where all sites are unoccupied (i.e., cooperatively binds). Because when all three sites are occupied by R, the transcription is suppressed (Fig. 1A, gray box), the transcriptional activity is the probability that at least one site is unoccupied by R at the steady state. The probability can be calculated from the chemical master equation (CME) governing the system with

respect to the effective total number of the repressor $\widetilde{R_T} = R_T/K_r$, where R_T is the total number of repressors (Table S1; see the Methods).

The transcription is turned on with a high probability when $\widetilde{R_T}$ is low, referred to as the transcriptional activation phase (TAP). As $\widetilde{R_T}$ increases, the probability decreases to zero, reaching to the transcriptional repression phase (TRP; Fig. 1B). The sharpness of this transition from transcriptional activation during TAP to repression during TRP depends on the cooperativity c. Specifically, when there is no cooperativity (i.e., $c = 1$), the transition shows a similar sensitivity with the Michaelis-Menten equation (Fig. 1B, red line). In contrast, when repressors bind cooperatively (i.e., $c < 1$), the sensitivity of the transition increases (Fig. 1B, blue line). This sensitivity can be quantified using the effective Hill coefficient $\log 81 / \log(EC_{10}/EC_{90})$, where EC_{90} and EC_{10} are the values of $\widetilde{R_T}$ at which the transcriptional activity becomes 0.9 and 0.1, respectively [1]. The measured effective Hill coefficients in the presence and absence of cooperativity are about 3 and 1.3, respectively (Fig. 1B).

Next, we simulated the time series of mRNA during TAP and TRP using the Gillespie algorithm. We chose the values of $\widetilde{R_T}$ at EC_{90} and EC_{10}, for TAP and TRP, respectively. In the absence of cooperativity, the timeseries of mRNA slightly fluctuate around their high average during TAP (Fig. 1C) and around their low average during TRP (Fig. 1D). However, in the presence of cooperativity, the timeseries of mRNA often drop to zero even during TAP (Fig. 1E), and conversely often lift up to high levels even during TRP (Fig. 1F). These undesired transcriptional states, arising due to noise, persists because transition between the transcriptional activation and repression occurs rarely due to cooperative binding [5]. As a result, cooperativity increases the variance in the number of mRNA, yielding a much higher Fano factor compared to the absence of cooperativity (Fig. 1G and Table S1).

2.2. Noise turns on the sequestration-based switch during TRP.

The transcriptional repression can occur not only through direct binding to DNA, but also by indirectly inhibiting the transcriptional activator that promotes transcription. Among indirect repression mechanisms, the sequestration has been identified to generate ultrasensitivity [21-24]. To investigate

whether this switch is robust to noise, we constructed a model describing the sequestration (Fig. 2A). In the model, the free activator (A) binds to the free DNA (E_F) with a dissociation constant of K_a to form the activated DNA (E_A). The transcription is inhibited as the free repressor (R) binds to A to form an inactive complex (R_A) with a dissociation constant of K_s (i.e., sequestration; Fig. 2A, gray box). Thus, the transcriptional activity is defined as the probability that the DNA is activated by the binding of A, not sequestered by R at the steady state. We derived the probability as a function of $\widetilde{R_T} = R_T/A_T$, the molar ratio between total numbers of the activator ($A_T = A + R_A + E_A$) and the repressor ($R_T = R + R_A$) with two scaled parameters $\widetilde{K_a} = K_a/A_T$ and $\widetilde{K_s} = K_s/A_T$ (Table S1; see Method for details).

The transcription turns on and off, respectively, when the molar ratio $\widetilde{R_T}$ is either below (TAP) or above one (TRP). The transition between transcriptional activation during TAP and repression during TRP becomes more sensitive as the binding between A and the DNA becomes stronger (i.e., $\widetilde{K_a}$ decreases; Fig. 2B). This is because strong activator (i.e., small $\widetilde{K_a}$) can promote the transcription even with a small number of activators, sustaining transcriptional activation during TAP as long as there are more activators than repressors (i.e., $\widetilde{R_T} < 1$; Fig. 2B, blue line). However, when the molar ratio exceeds one (i.e., $\widetilde{R_T} > 1$; Fig. 2B), the majority of A is sequestered by R. As a result, a sensitive transition from TAP to TRP occurs near $\widetilde{R_T} = 1$ with the high effective Hill coefficient of about 50. On the other hand, the transition occurs gradually with the effective Hill coefficient of about 2 in the case of weak activator (i.e., large $\widetilde{K_a}$; Fig. 2B, red line).

Next, we simulated the timeseries of activated DNA and mRNA at the value of $\widetilde{R_T} = 10^{0.5}$ in TRP (Fig. 2B, orange star). For a weak activator, the activated DNA indued by noise is swiftly restored to the repressed state, keeping the number of mRNA consistently low around zero (Fig. 2C). On the other hand, for a strong activator, this undesired activation of DNA during TRP persists over a long period, leading to a significant increase in the number of mRNA (Fig. 2D). This disparity arises when a sequestered A is released from R and binds with the DNA despite of being TRP (unexpected activation; Fig. 2E). Then, a week activator quickly dissociates from the DNA itself and thus the transcription is turned off to its original state (Fig. 2E, red arrow). Meanwhile, a strong activator remains bound to the DNA for a long time (Fig. 2E, blue arrow). As a result, the undesired transcriptional activation persists even during TRP, resulting in a considerable increase in the number of mRNA. This leads to a bimodal

140 distribution of mRNA molecules deviating substantially from a Poisson distribution, with a strong
141 activator (Fig. 2F, blue bars) unlike a weak activator (Fig. 2F, red bars). Thus, a strong activator yields
142 much higher transcriptional noise compared to a weak activator during TRP (Fig. 2G). In conclusion,
143 when the binding between the activator and DNA is tight, a sensitive transcriptional response can be
144 generated with the sole sequestration. However, this tight binding leads to high transcriptional noise as
145 the undesired transcriptional activation during TRP persists for a long period.

146

147 **2.3. Noise turns off the sequestration and blocking-based switch during TAP**

148 When transcription is regulated by the sole sequestration, high transcriptional noise occurs
149 during TRP due to the absence of repression for the activator bound on DNA. This DNA-bound-activator
150 can be suppressed when the repressor blocks the transcription by forming a complex with the DNA-
151 bound-activator (i.e., blocking) or pulls off the activator from the DNA (i.e., displacement). Indeed, these
152 repression mechanisms are commonly employed in addition to the sole sequestration in many biological
153 systems [7, 14]. We first added the blocking to the sole sequestration model, where the repressor (R)
154 can directly bind to the DNA-bound-activator (E_A) with a dissociation constant of K_b to form the
155 repressed DNA (E_R; Fig. 3A, gray box). Based on this model, we derived the transcriptional activity as
156 function of the molar ratio $\widetilde{R_T}$ with three scaled parameters $\widetilde{K_a} = K_a/A_T$, $\widetilde{K_s} = K_s/A_T$ and $\widetilde{K_b} = K_b/A_T$
157 (Table S1; see Method for details). The derived transcriptional activity exhibits a high sensitivity of
158 response to changes in $\widetilde{R_T}$ (i.e., the effective Hill coefficient of about 50; Fig. 3B). Furthermore, the
159 addition of blocking rapidly restores the undesired activation of DNA during TRP to the repressed state
160 (Fig. 3C, top panel). This is evident in the simulated timeseries of mRNA, which remain close to zero,
161 without sharp increase of mRNA (Fig. 3C, bottom right panel) unlike the sole sequestration (Fig. 3C,
162 bottom left panel). That is, the transcription triggered by noise-induced activator binding to DNA during
163 TRP is immediately inhibited by the repressor via blocking (Fig. 3D, blue arrow) in contrast to the sole
164 sequestration (Fig. 3D, red arrow). As a result, in the presence of the blocking, the distribution of mRNA
165 molecules is concentrated near zero (Fig. 3E, blue bars) rather than bimodal (Fig. 3E, red bars),
166 reducing the transcriptional noise during TRP (Fig. 3F and Table S1).

However, the addition of blocking dramatically increases the transcriptional noise during TAP (Fig. 3F). To investigate the source of such high transcriptional noise during TAP, we simulated the timeseries of non-activated DNA and mRNA at the value of $\widetilde{R_T} = 10^{-0.1}$ in TAP (Fig. 3C, gray star). In the case of the sole sequestration, non-activated DNA is restored to the activated state rapidly (Fig. 3G, top left panel), and thus the timeseries of mRNA maintain their high average during TAP (Fig. 3G, bottom left panel). In contrast, when the blocking is added, this undesired repression during TAP persists for a long period (Fig. 3G, top right panel), causing a dramatic reduction in the number of mRNA (Fig. 3G, bottom right panel). This significant reduction arises when the repressor, released from the activator due to noise, binds with the activator bound to DNA during TAP (unexpected repression; Fig. 3H). Then, the repressor remains bound until it unbinds from DNA-bound-activator itself (Fig. 3H). This causes a dramatic reduction in the number of mRNA even during TAP, leading to a small additional peak around zero in the mRNA distribution (Fig. 3I). Due to the bimodality, the transcriptional noise surges during TAP (Fig. 3F).

2.4. The sequestration, blocking, and displacement-based switch is robust to noise

In the presence of blocking, the undesired repression during TAP stems from the unexpected binding of the repressor to the activator on DNA. This can be prevented by the addition of displacement, which facilitates dissociation of the DNA-bound repressor-activator complex from the DNA. To investigate this, we incorporated the displacement into the blocking and sequestration model. In this model, the repressor-activator complex (R_A) can dissociate from the DNA with a dissociation constant of K_d (Fig. 4A, gray box). We derived the transcriptional activity as the function of the molar ratio $\widetilde{R_T}$ with four scaled parameters $\widetilde{K_a} = K_a/A_T$, $\widetilde{K_s} = K_s/A_T$, $\widetilde{K_b} = K_b/A_T$ and $\widetilde{K_d} = K_d/A_T$ (Table S1; see Methods for details). The transcriptional activity can exhibit an ultrasensitive response to changes in $\widetilde{R_T}$ with the effective Hill coefficient of about 200 (Fig. 4B, blue and red lines).

Furthermore, the addition of displacement rapidly restores the undesired repression of DNA during TAP to the activated state (Fig. 4C, top panel). This is evident in the simulated timeseries of mRNA, which do not drop to zero (Fig. 4C, bottom right panel) unlike the combination of the

194 sequestration and blocking. That is, when a repressor binds to the DNA-bound-activator due to noise
195 during TAP (unexpected repression; Fig. 4), repressor-activator complex is immediately released from
196 DNA via displacement (Fig. 4D, blue arrow). This does not happen without displacement (Fig. 4D, red
197 arrow). Taken together, the inclusion of displacement eliminates the additional peak near zero seen in
198 the sequestration and blocking model (Fig. 4E), leading to a reduction in transcriptional noise during
199 TAP (Fig. 4F and Table S1).

200

201 **3. Discussion**

202 Traditionally, ultrasensitive transcriptional responses are generated by cooperative binding of
203 transcriptional repressors to multiple DNA sites. This mechanism can trigger a sharp transcriptional
204 transition from transcriptional repression during TRP to activation during TAP as the number of
205 repressors surpasses a threshold. However, the presence of noise can lead to prolonged periods of
206 undesired repression and activation during TAP and TRP, respectively (Fig. 1). Thus, we have shifted
207 our focus from direct repression—where repressors directly bind to DNA, as seen in cooperative binding
208 to multiple DNA sites—to the realm of indirect transcriptional repression: sequestration, blocking, and
209 displacement. Sequestration alone can generate an ultrasensitive response that is attuned to changes
210 in the molar ratio between repressors and activators. Specifically, when the number of repressors falls
211 short of that of activators (i.e., the molar ratio is less than one), an unsequestered activator binds to
212 DNA, thereby promoting transcription. As the molar ratio surpasses one, a majority of activators become
213 sequestered by repressors, promoting a sharp transition to transcriptional inhibition (Fig. 2).
214 Furthermore, the transcriptional repression (activation) during TRP (TAP) can be stably maintained by
215 blocking (displacement) even in the presence of noise. Specifically, when an activator, unexpectedly
216 released from repressors, binds to DNA and initiates transcription during TRP (Fig. 2), the activator is
217 immediately blocked by a repressor, resulting in the prompt restoration of transcriptional repression (Fig.
218 3). When a repressor unexpectedly blocks an activator that is already bound to DNA during TAP, the
219 repressor-activator complex is displaced, swiftly reinitiating transcriptional activation (Fig. 4). Taken
220 together, our exploration has unveiled an ultrasensitive transcriptional switch endowed with resilience

221 against noise during both TAP and TRP. This breakthrough holds the potential to enhance the stability
222 and reliability of transcriptional regulation within intricate biological systems.

223 Interestingly, although two models with or without a particular repression mechanism may
224 appear similar in deterministic simulations, they can behave quite differently in stochastic simulations.
225 Specifically, in the deterministic ODE, where the transcription of mRNA is proportional to the
226 transcriptional activity, two models exhibiting similar transcriptional activity yield indistinguishable
227 behaviors of mRNA [14]. On the other hand, in the stochastic models, the distributions of mRNA can
228 be completely different despite resembling transcriptional activities. For example, all transcriptional
229 activity of each model shows similar responses with respect to changes in the molar ratio (Fig. 3B and
230 4B), whereas their Fano factors are completely different (Fig. 3F and 4F). Therefore, a comprehensive
231 understanding of the precise repression mechanism is essential to ensure unbiased modeling results
232 when considering the presence of noise.

233 Biological oscillators and biological switches require ultrasenstivity to generate strong rhythms
234 [24, 25] and bistable responses [2], respectively. In addition to the ultrasenstivity, these systems need
235 to exhibit robustness against intrinsic noise to ensure accurate timing and precise decision-making.
236 Indeed, such biological systems that require both ultrasensitivity and precision employ the multiple
237 repression mechanisms. For instance, the MDM2-p53 oscillator is known to utilize the blocking and
238 displacement to inhibit p53 by MDM2 [26, 27]. Similarly, the NF-kB oscillator, and circadian clocks in
239 mammals and Drosophila employ a combination of the sequestration, blocking, and displacement [13,
240 15-19]. Moreover, the Rb-EF bistable switches in the cell cycle incorporates the blocking and chromatin
241 structure modification [28-30]. Our work highlights the significance of the multiple repression
242 mechanisms in achieving robust and precise regulatory outcomes in these systems.

243

244 4. Methods

245 We used a approach established by A. Sanchez et al [5] to calculate the transcriptional activity
246 and the Fano factor for the number of mRNA (see SI for details). The results are summarized in Table
247 S1. The transcriptional activity is the probability that the transcription of DNA is activated. The

transcriptional activity and Fano factors of all models depending on the scaled repressor level ($\widetilde{R_T}$). Specifically, the transcriptional activity ($TA(\widetilde{R_T})$; Fig. 1B) and Fano factor ($FF(\widetilde{R_T})$; Fig. 1G) for the three binding sites model with cooperativity (Fig. 1A) depend on the effective total repressor $\widetilde{R_T} = R_T/K_r$, where R_T is the total number of repressors and K_r is the dissociation constant between repressor and binding sites on DNA:

$$TA(\widetilde{R_T}) = 1 - \frac{\widetilde{R_T}^3}{c^3 + 3c^3\widetilde{R_T} + 3c^2\widetilde{R_T}^2 + \widetilde{R_T}^3},$$

and

$$FF(\widetilde{R_T}) = 1 + \frac{\tilde{\alpha}\widetilde{R_T}^4\left[3(\tilde{\beta}+2)(\tilde{\beta}+3)\widetilde{R_T}^4+\left[3c\tilde{\beta}^2+(24c+3)\tilde{\beta}+45c\right]\widetilde{R_T}^3+\left[c\tilde{\beta}^2+3c(2c+3)\tilde{\beta}+2c(9c+10)\right]\widetilde{R_T}^2+c\left[(1+2c)\tilde{\beta}+(1+12c)\right]\widetilde{R_T}+2c^2\right]}{\begin{aligned}&3(\tilde{\beta}+1)(\tilde{\beta}+2)(\tilde{\beta}+3)\widetilde{R_T}^8+3\left[c(3c+1)\tilde{\beta}^3+(21c^2+8c+1)\tilde{\beta}^2+(48c^2+17c+1)\tilde{\beta}+6c(1+6c)\right]\widetilde{R_T}^7\\&+c\left[6(1+36c^2+27c^3)+(20+36c+315c^2+135c^3)\tilde{\beta}+3(3+5c+45c^2+9c^3)\tilde{\beta}^2+(1+18c^2)\tilde{\beta}^3\right]\widetilde{R_T}^6\\&+c\left[3c^2(3c+2)\tilde{\beta}^3+(54c^4+90c^3+57c^2+2c+1)\tilde{\beta}^2+(324c^4+252c^3+126c^2+12c+1)\tilde{\beta}+18c^2(27c^2+6c+4)\right]\widetilde{R_T}^5\\&+c^2\left[6c^2\tilde{\beta}^3+3c(9c^3+12c^2+19c+2)\tilde{\beta}^2+(243c^4+198c^3+153c^2+9c+2)\tilde{\beta}+18c^2(27c^2+9c+4)\right]\widetilde{R_T}^4\\&+c^4\left[\tilde{\beta}^3+6(3c^2+2c+2)\tilde{\beta}^2+(54c^3+153c^2+72c+29)\tilde{\beta}+6(27c^3+54c^2+2)\right]\widetilde{R_T}^3\\&+c^4\left[(3c^2+2c+1)\tilde{\beta}^2+(36c^3+33c^2+18c+1)\tilde{\beta}+54c^2(1+3c)\right]\widetilde{R_T}^2+c^5\left[(6c^2+3c+2)\tilde{\beta}+54c^2\right]\widetilde{R_T}+6c^7\end{aligned}},$$

where $\tilde{\alpha}$ is the scaled production rate of mRNA, $\tilde{\beta}$ is the scaled production rate of mRNA, and c is cooperativity between binding sites (Fig. 1B).

The transcriptional activity (Fig. 2B) and Fano factor (Fig. 2G) for the model describing the sequestration (Fig. 2) depends on the molar ratio $\widetilde{R_T} = R_T/A_T$ between the total numbers of repressors (R_T) and activators (A_T):

$$TA(\widetilde{R_T}) = \frac{\tilde{A}(\widetilde{R_T}, \widetilde{K_s})/\widetilde{K_a}}{1 + \tilde{A}(\widetilde{R_T}, \widetilde{K_s})/\widetilde{K_a}},$$

and

$$FF(\widetilde{R_T}) = 1 + \frac{\tilde{\alpha}}{\left(1 + \tilde{A}(\widetilde{R_T}, \widetilde{K_s})/\widetilde{K_a}\right)\left(\tilde{A}(\widetilde{R_T}, \widetilde{K_s}) + \widetilde{K_a} + \tilde{\beta}\right)},$$

where $\tilde{A}(\widetilde{R_T}, \widetilde{K_s}) = \frac{1-\widetilde{R_T}-\widetilde{K_s}+\sqrt{(1-\widetilde{R_T}-\widetilde{K_s})^2+4\widetilde{K_s}}}{2}$ is the fraction of free activator among total activator, and $\widetilde{K_s}$ and $\widetilde{K_a}$ are the scaled dissociation constants between repressor and activator and between activator and DNA, respectively.

The transcriptional activity (Fig. 3B) and Fano factor (Fig. 3F) for the model describing the sequestration and blocking (Fig. 3) depends on the molar ratio $\widetilde{R_T}$:

$$TA\left(\widetilde{R_T}\right) = \frac{\frac{\tilde{A}\left(\widetilde{R_T},\widetilde{K_s}\right)}{\widetilde{K_a}}}{1+\frac{\tilde{A}\left(\widetilde{R_T},\widetilde{K_s}\right)}{\widetilde{K_a}}+\frac{\tilde{A}\left(\widetilde{R_T},\widetilde{K_s}\right)}{\widetilde{K_a}}\frac{\tilde{R}\left(\widetilde{R_T},\widetilde{K_s}\right)}{\widetilde{K_b}}},$$

and

$$FF\left(\widetilde{R_T}\right) = 1 + \frac{\tilde{\alpha}\left[\widetilde{K_b}+\tilde{\beta}+\left(\tilde{A}\left(\widetilde{R_T},\widetilde{K_s}\right)+\tilde{\beta}\right)\frac{\tilde{A}\left(\widetilde{R_T},\widetilde{K_s}\right)}{\widetilde{K_a}}\frac{\tilde{R}\left(\widetilde{R_T},\widetilde{K_s}\right)}{\widetilde{K_b}}\right]}{\left(1+\frac{\tilde{A}\left(\widetilde{R_T},\widetilde{K_s}\right)}{\widetilde{K_a}}+\frac{\tilde{A}\left(\widetilde{R_T},\widetilde{K_s}\right)}{\widetilde{K_a}}\frac{\tilde{R}\left(\widetilde{R_T},\widetilde{K_s}\right)}{\widetilde{K_b}}\right)\left[\widetilde{K_a}\left(\widetilde{K_b}+\tilde{\beta}\right)+\left(\tilde{A}\left(\widetilde{R_T},\widetilde{K_s}\right)+\tilde{\beta}\right)\left(\tilde{R}\left(\widetilde{R_T},\widetilde{K_s}\right)+\widetilde{K_b}+\tilde{\beta}\right)\right]},$$

where $\tilde{R}\left(\widetilde{R_T},\widetilde{K_s}\right) = \frac{\widetilde{R_T}-1-\widetilde{K_s}+\sqrt{\left(1-\widetilde{R_T}-\widetilde{K_s}\right)^2+4\widetilde{K_s}}}{2}$ is the fraction of free repressor to the total activator and $\widetilde{K_b}$ is the scaled dissociation constant between repressor and DNA-bound-activator.

The transcriptional activity (Fig. 4B) and Fano factor (Fig. 4F) for the model describing the sequestration, blocking, and displacement (Fig. 4) depends on the molar ratio $\widetilde{R_T}$:

$$TA\left(\widetilde{R_T}\right) = \frac{\tilde{I}\left(\widetilde{R_T},\widetilde{K_a},\widetilde{K_s}\right)\frac{\tilde{A}\left(\widetilde{R_T},\widetilde{K_s}\right)}{\widetilde{K_a}}}{1+\tilde{I}\left(\widetilde{R_T},\widetilde{K_a},\widetilde{K_s}\right)\frac{\tilde{A}\left(\widetilde{R_T},\widetilde{K_s}\right)}{\widetilde{K_a}}+\tilde{J}\left(\widetilde{R_T},\widetilde{K_a},\widetilde{K_s}\right)\frac{\tilde{A}\left(\widetilde{R_T},\widetilde{K_s}\right)}{\widetilde{K_a}}\frac{\tilde{R}\left(\widetilde{R_T},\widetilde{K_s}\right)}{\widetilde{K_b}}},$$

and

$$FF\left(\widetilde{R_T}\right) = 1 + \frac{\tilde{\alpha}\left[\left(\widetilde{R_A}\left(\widetilde{R_T},\widetilde{K_s}\right)+\widetilde{K_b}+\widetilde{K_d}+\tilde{\beta}\right)+\left(1+\widetilde{K_d}+\tilde{\beta}\right)\tilde{J}\left(\widetilde{R_T},\widetilde{K_a},\widetilde{K_s}\right)\frac{\tilde{A}\left(\widetilde{R_T},\widetilde{K_s}\right)}{\widetilde{K_a}}\frac{\tilde{R}\left(\widetilde{R_T},\widetilde{K_s}\right)}{\widetilde{K_b}}\right]}{\left(1+\tilde{I}\left(\widetilde{R_T},\widetilde{K_a},\widetilde{K_s}\right)\frac{\tilde{A}\left(\widetilde{R_T},\widetilde{K_s}\right)}{\widetilde{K_a}}+\tilde{J}\left(\widetilde{R_T},\widetilde{K_a},\widetilde{K_s}\right)\frac{\tilde{A}\left(\widetilde{R_T},\widetilde{K_s}\right)}{\widetilde{K_a}}\frac{\tilde{R}\left(\widetilde{R_T},\widetilde{K_s}\right)}{\widetilde{K_b}}\right)\left[\left(\widetilde{K_b}+\widetilde{K_d}+\tilde{\beta}\right)\left(\tilde{A}\left(\widetilde{R_T},\widetilde{K_s}\right)+\widetilde{K_a}+\tilde{\beta}\right)+\left(\widetilde{K_b}+\widetilde{K_a}+\tilde{\beta}\right)\widetilde{R_A}\left(\widetilde{R_T},\widetilde{K_s}\right)+\left(1+\widetilde{K_d}+\tilde{\beta}\right)\tilde{R}\left(\widetilde{R_T},\widetilde{K_s}\right)\right]},$$

where $\tilde{I}\left(\widetilde{R_T},\widetilde{K_a},\widetilde{K_s}\right) = \frac{\widetilde{K_s}+\sigma\widetilde{K_a}+\tilde{R}\left(\widetilde{R_T},\widetilde{K_s}\right)}{\widetilde{K_s}+\sigma\widetilde{K_a}+\sigma\tilde{R}\left(\widetilde{R_T},\widetilde{K_s}\right)}$, $\tilde{J}\left(\widetilde{R_T},\widetilde{K_a},\widetilde{K_s}\right) = \frac{\widetilde{K_s}+\sigma\widetilde{K_a}+\sigma\tilde{R}\left(\widetilde{R_T},\widetilde{K_s}\right)}{\widetilde{K_s}+\sigma\widetilde{K_a}+\sigma\tilde{R}\left(\widetilde{R_T},\widetilde{K_s}\right)}$, $\sigma = \frac{\widetilde{K_s}\widetilde{K_d}}{\widetilde{K_a}\widetilde{K_b}}$, and $\widetilde{K_d}$ is the scaled dissociation constant between repressor-activator complex and DNA.

Data availability

The datasets used and/or analyzed during the current study available from the corresponding author on reasonable request.

Code availability

The underlying code for this study is not publicly available but may be made available to qualified researchers on reasonable request from the corresponding author.

References

1. Ferrell JE, Jr., Ha SH. Ultrasensitivity part I: Michaelian responses and zero-order ultrasensitivity. Trends Biochem Sci. 2014;39(10):496-503. Epub 2014/09/23. doi: 10.1016/j.tibs.2014.08.003. PubMed PMID: 25240485; PubMed Central PMCID: PMCPMC4214216.
2. Ferrell JE, Jr., Ha SH. Ultrasensitivity part III: cascades, bistable switches, and oscillators. Trends Biochem Sci. 2014;39(12):612-8. Epub 2014/12/03. doi: 10.1016/j.tibs.2014.10.002. PubMed PMID: 25456048; PubMed Central PMCID: PMCPMC4254632.
3. Zhang Q, Bhattacharya S, Andersen ME. Ultrasensitive response motifs: basic amplifiers in molecular signalling networks. Open Biol. 2013;3(4):130031. Epub 20130424. doi: 10.1098/rsob.130031. PubMed PMID: 23615029; PubMed Central PMCID: PMCPMC3718334.
4. Lu MS, Mauser JF, Prehoda KE. Ultrasensitive synthetic protein regulatory networks using mixed decoys. ACS Synth Biol. 2012;1(2):65-72. doi: 10.1021/sb200010w. PubMed PMID: 22639735; PubMed Central PMCID: PMCPMC3358930.
5. Sanchez A, Garcia HG, Jones D, Phillips R, Kondev J. Effect of promoter architecture on the cell-to-cell variability in gene expression. PLoS Comput Biol. 2011;7(3):e1001100. Epub 20110303. doi: 10.1371/journal.pcbi.1001100. PubMed PMID: 21390269; PubMed Central PMCID: PMCPMC3048382.
6. Dey S, Soltani M, Singh A. Enhancement of gene expression noise from transcription factor binding to genomic decoy sites. Sci Rep. 2020;10(1):9126. Epub 20200604. doi: 10.1038/s41598-020-65750-2. PubMed PMID: 32499583; PubMed Central PMCID: PMCPMC7272470.
7. Gaston K, Jayaraman PS. Transcriptional repression in eukaryotes: repressors and repression mechanisms. Cell Mol Life Sci. 2003;60(4):721-41. Epub 2003/06/06. doi: 10.1007/s00018-003-2260-3. PubMed PMID: 12785719.
8. Renkawitz R. Transcriptional repression in eukaryotes. Trends Genet. 1990;6(6):192-7. Epub 1990/06/01. doi: 10.1016/0168-9525(90)90176-7. PubMed PMID: 2196723.
9. Benezra R, Davis RL, Lockshon D, Turner DL, Weintraub H. The protein Id: a negative regulator of helix-loop-helix DNA binding proteins. Cell. 1990;61(1):49-59. doi: 10.1016/0092-8674(90)90214-y. PubMed PMID: 2156629.
10. Van Doren M, Ellis HM, Posakony JW. The Drosophila extramacrochaetae protein antagonizes sequence-specific DNA binding by daughterless/achaete-scute protein complexes. Development. 1991;113(1):245-55. doi: 10.1242/dev.113.1.245. PubMed PMID: 1764999.
11. Chadsey MS, Karlinsey JE, Hughes KT. The flagellar anti-sigma factor FlgM actively dissociates Salmonella typhimurium sigma28 RNA polymerase holoenzyme. Genes Dev. 1998;12(19):3123-36. doi: 10.1101/gad.12.19.3123. PubMed PMID: 9765212; PubMed Central PMCID: PMCPMC317189.
12. Jayaraman PS, Hirst K, Goding CR. The activation domain of a basic helix-loop-helix protein is masked by repressor interaction with domains distinct from that required for transcription regulation. EMBO J. 1994;13(9):2192-9. Epub 1994/05/01. PubMed PMID: 8187772; PubMed Central PMCID: PMCPMC395073.
13. Potoyan DA, Zheng W, Komives EA, Wolynes PG. Molecular stripping in the NF-kappaB/IkappaB/DNA genetic regulatory network. Proc Natl Acad Sci U S A. 2016;113(1):110-5. Epub 2015/12/25. doi: 10.1073/pnas.1520483112. PubMed PMID: 26699500; PubMed Central PMCID: PMCPMC4711861.
14. Jeong EM, Song YM, Kim JK. Combined multiple transcriptional repression mechanisms generate ultrasensitivity and oscillations. Interface Focus. 2022;12(3):20210084. Epub

20220415. doi: 10.1098/rsfs.2021.0084. PubMed PMID: 35450279; PubMed Central PMCID: PMCPMC9010851.

15. Bergqvist S, Alverdi V, Mengel B, Hoffmann A, Ghosh G, Komives EA. Kinetic enhancement of NF-kappaBxDNA dissociation by IkappaBalpha. Proc Natl Acad Sci U S A. 2009;106(46):19328-33. Epub 2009/11/06. doi: 10.1073/pnas.0908797106. PubMed PMID: 19887633; PubMed Central PMCID: PMCPMC2780789.

16. Menet JS, Abruzzi KC, Desrochers J, Rodriguez J, Rosbash M. Dynamic PER repression mechanisms in the Drosophila circadian clock: from on-DNA to off-DNA. Genes Dev. 2010;24(4):358-67. Epub 2010/02/18. doi: 10.1101/gad.1883910. PubMed PMID: 20159956; PubMed Central PMCID: PMCPMC2816735.

17. Cao X, Yang Y, Selby CP, Liu Z, Sancar A. Molecular mechanism of the repressive phase of the mammalian circadian clock. Proc Natl Acad Sci U S A. 2021;118(2). Epub 2021/01/15. doi: 10.1073/pnas.2021174118. PubMed PMID: 33443219; PubMed Central PMCID: PMCPMC7812753.

18. Chiou YY, Yang Y, Rashid N, Ye R, Selby CP, Sancar A. Mammalian Period represses and de-represses transcription by displacing CLOCK-BMAL1 from promoters in a Cryptochrome-dependent manner. Proc Natl Acad Sci U S A. 2016;113(41):E6072-E9. Epub 2016/10/01. doi: 10.1073/pnas.1612917113. PubMed PMID: 27688755; PubMed Central PMCID: PMCPMC5068302.

19. Ye R, Selby CP, Chiou YY, Ozkan-Dagliyan I, Gaddameedhi S, Sancar A. Dual modes of CLOCK:BMAL1 inhibition mediated by Cryptochrome and Period proteins in the mammalian circadian clock. Genes Dev. 2014;28(18):1989-98. Epub 2014/09/18. doi: 10.1101/gad.249417.114. PubMed PMID: 25228643; PubMed Central PMCID: PMCPMC4173159.

20. Ferrell JE, Jr., Ha SH. Ultrasensitivity part II: multisite phosphorylation, stoichiometric inhibitors, and positive feedback. Trends Biochem Sci. 2014;39(11):556-69. Epub 20141023. doi: 10.1016/j.tibs.2014.09.003. PubMed PMID: 25440716; PubMed Central PMCID: PMCPMC4435807.

21. Buchler NE, Cross FR. Protein sequestration generates a flexible ultrasensitive response in a genetic network. Mol Syst Biol. 2009;5:272. Epub 2009/05/21. doi: 10.1038/msb.2009.30. PubMed PMID: 19455136; PubMed Central PMCID: PMCPMC2694680.

22. Buchler NE, Louis M. Molecular titration and ultrasensitivity in regulatory networks. J Mol Biol. 2008;384(5):1106-19. Epub 2008/10/22. doi: 10.1016/j.jmb.2008.09.079. PubMed PMID: 18938177.

23. Kim JK, Forger DB. A mechanism for robust circadian timekeeping via stoichiometric balance. Mol Syst Biol. 2012;8:630. Epub 2012/12/06. doi: 10.1038/msb.2012.62. PubMed PMID: 23212247; PubMed Central PMCID: PMCPMC3542529.

24. Kim JK. Protein sequestration versus Hill-type repression in circadian clock models. IET Syst Biol. 2016;10(4):125-35. Epub 2016/07/23. doi: 10.1049/iet-syb.2015.0090. PubMed PMID: 27444022.

25. Novak B, Tyson JJ. Design principles of biochemical oscillators. Nat Rev Mol Cell Biol. 2008;9(12):981-91. Epub 2008/10/31. doi: 10.1038/nrm2530. PubMed PMID: 18971947; PubMed Central PMCID: PMCPMC2796343.

26. Cross B, Chen L, Cheng Q, Li B, Yuan ZM, Chen J. Inhibition of p53 DNA binding function by the MDM2 protein acidic domain. J Biol Chem. 2011;286(18):16018-29. Epub 2011/04/02. doi: 10.1074/jbc.M111.228981. PubMed PMID: 21454483; PubMed Central PMCID: PMCPMC3091211.

27. Chen J. The Cell-Cycle Arrest and Apoptotic Functions of p53 in Tumor Initiation and Progression. Cold Spring Harb Perspect Med. 2016;6(3):a026104. Epub 2016/03/05. doi: 10.1101/cshperspect.a026104. PubMed PMID: 26931810; PubMed Central PMCID: PMCPMC4772082.

28. Nevins JR. E2F: a link between the Rb tumor suppressor protein and viral oncoproteins. Science. 1992;258(5081):424-9. Epub 1992/10/16. doi: 10.1126/science.1411535. PubMed PMID: 1411535.

29. Yao G, Lee TJ, Mori S, Nevins JR, You L. A bistable Rb-E2F switch underlies the restriction point. Nat Cell Biol. 2008;10(4):476-82. Epub 20080323. doi: 10.1038/ncb1711. PubMed PMID: 18364697.

30. Dimova DK, Dyson NJ. The E2F transcriptional network: old acquaintances with new faces. Oncogene. 2005;24(17):2810-26. doi: 10.1038/sj.onc.1208612. PubMed PMID: 15838517.

Acknowledgement

This study was funded by Institute for Basic Science (IBS-R029-C3) (J.K.K.), and the Human Frontiers Science Program Organization (RGY0063/2017) (J.K.K.). The funder played no role in study design, data collection, analysis and interpretation of data, or writing of this manuscript.

Authors Contribution

All authors provided conceptualization of the manuscript, performed visualization and formal analysis, participated in investigation, and wrote the paper. E.M.J. contributed to the methodology. J.K.K. acquired funding and supervised the work conducted here.

Competing Interests

All authors declare no financial or non-financial competing interests.

Supplementary Information

Supplementary tables: Table S1.

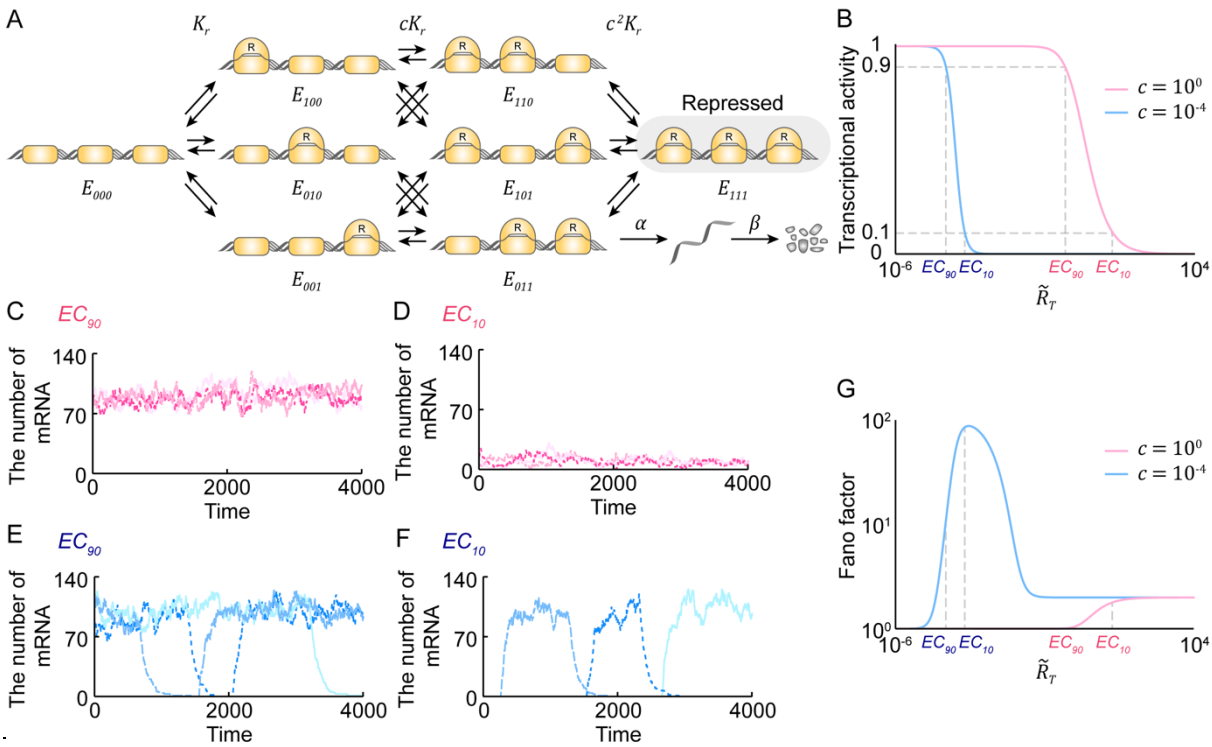

Figure 1. The transcriptional ultrasensitive switch based on cooperative binding suffers from undesired switch transition due to noise. (A) Schematic diagram of the model describing the binding of the repressor (R) to three sites on DNA. R can bind to an unoccupied site (E_{000}) with a dissociation constant of K_r. When one site is occupied (E_{001}, E_{010}, or E_{100}), R can bind to the other two sites with a dissociation constant of cK_r. When two sites are occupied (E_{110}, E_{101}, or E_{011}), R can bind to the remaining site with a dissociation constant of c^2K_r. Accordingly, when $c < 1$, cooperativity is present, while absent when $c = 1$. When all sites are occupied (E_{111}), the transcription is repressed (gray box); otherwise, mRNA is transcribed with the rate of α and decays with the rate of β. (B) Consequently, as the total effective number of the repressor ($\widetilde{R_T}$) increases, the probability that the transcription is activated (i.e., transcriptional activity) decreases, transitioning from transcriptional activation phase (TAP) to transcriptional repression phase (TRP). Such transition in the presence of cooperativity (blue line) is more sensitive to changes in $\widetilde{R_T}$ (i.e., a shorter distance between EC_{90} and EC_{10}) compared to in the absence of the cooperativity (red line). (C – D) In the absence of cooperativity, the simulated timeseries of mRNA fluctuate around their high and low averages during TAP (i.e., when $\widetilde{R_T}$ is at EC_{90}) (C) and during TRP (i.e., when $\widetilde{R_T}$ is at EC_{10}) (D), respectively. (E – F) On the other hand, in the presence of cooperativity, the number of mRNA can decrease to 0 even during TAP and can significantly increase even during TRP (F), respectively. (G) As a result, in the presence of cooperativity, the number of mRNA exhibits greater variance, resulting in a higher Fano factor compared to the absence of cooperativity.

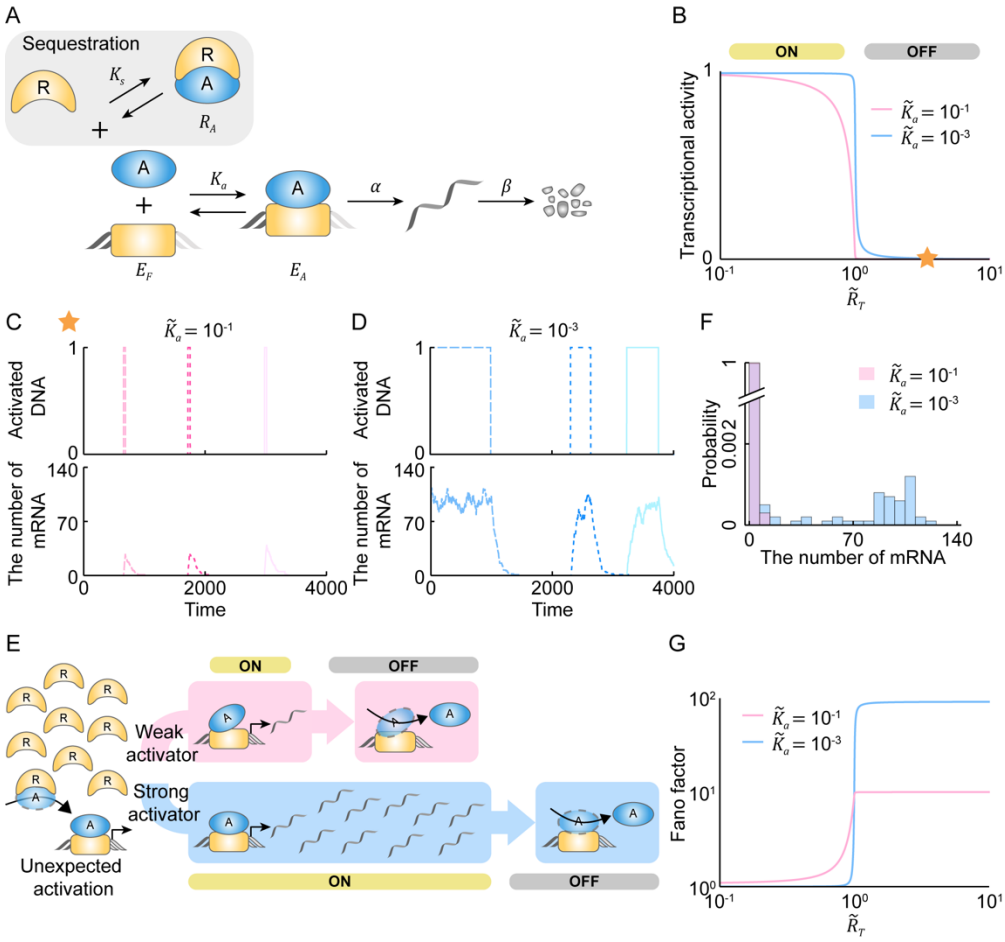

Figure 2. Transcriptional ultrasensitive switch based on the sole sequestration is sensitive to noise during TRP due to undesired transcriptional activation. (A) Schematic diagram of the model describing the sequestration. The binding of the activator (A) to the DNA (E_F) with a dissociation constant of K_a forms the activated DNA (E_A) to promote the transcription of mRNA with the rate of α, which decays with the rate of β. On the other hand, the binding of the repressor (R) to A with a dissociation constant of K_s leads to the transcriptional repression (i.e., sequestration; gray box). (B) Consequently, when the molar ratio $\widetilde{R_T} = R_T/A_T$ between the total activator (A_T) and repressor (R_T) is less than one (TAP), unsequestered activators can turn on transcription. In contrast, when the molar ratio exceeds one (TRP), almost all activators are sequestered by repressors, and thus transcription is turned off. As a result, around $\widetilde{R_T} = 1$, a sensitive transition from TAP to TRP occurs with respect to changes in $\widetilde{R_T}$. Notably, strong activators, which bind tightly to DNA, exhibit a more sensitive transition compared to weak activators that bind loosely. (C – D) The undesired activation is restored during TRP to the repressed state for a weak activator (C), unlike a strong activator (D). Here, the timeseries of activated DNA and mRNA are simulated at $\widetilde{R_T} = 10^{0.5}$ (orange star in (B)). (E) When noise-induced unbinding of A from the R_A complex occurs, the transcription can be turned on by binding for the A to DNA (i.e, unexpected activation occurs). Such undesired activation during TRP persists for a long time due to the tight binding of a strong activator (blue arrow), but not a weak activator (red arrow). This sharply increases the number of mRNA. (F) As a result, the stationary distribution of mRNA molecules shows an additional peak far from zero, leading to bimodality with a strong activator (blue bars) unlike a weak activator (red bars). (G) Such bimodality deviates the distribution from a Poisson distribution, resulting in a higher Fano factor for a strong activator compared to a weak activator during TRP.

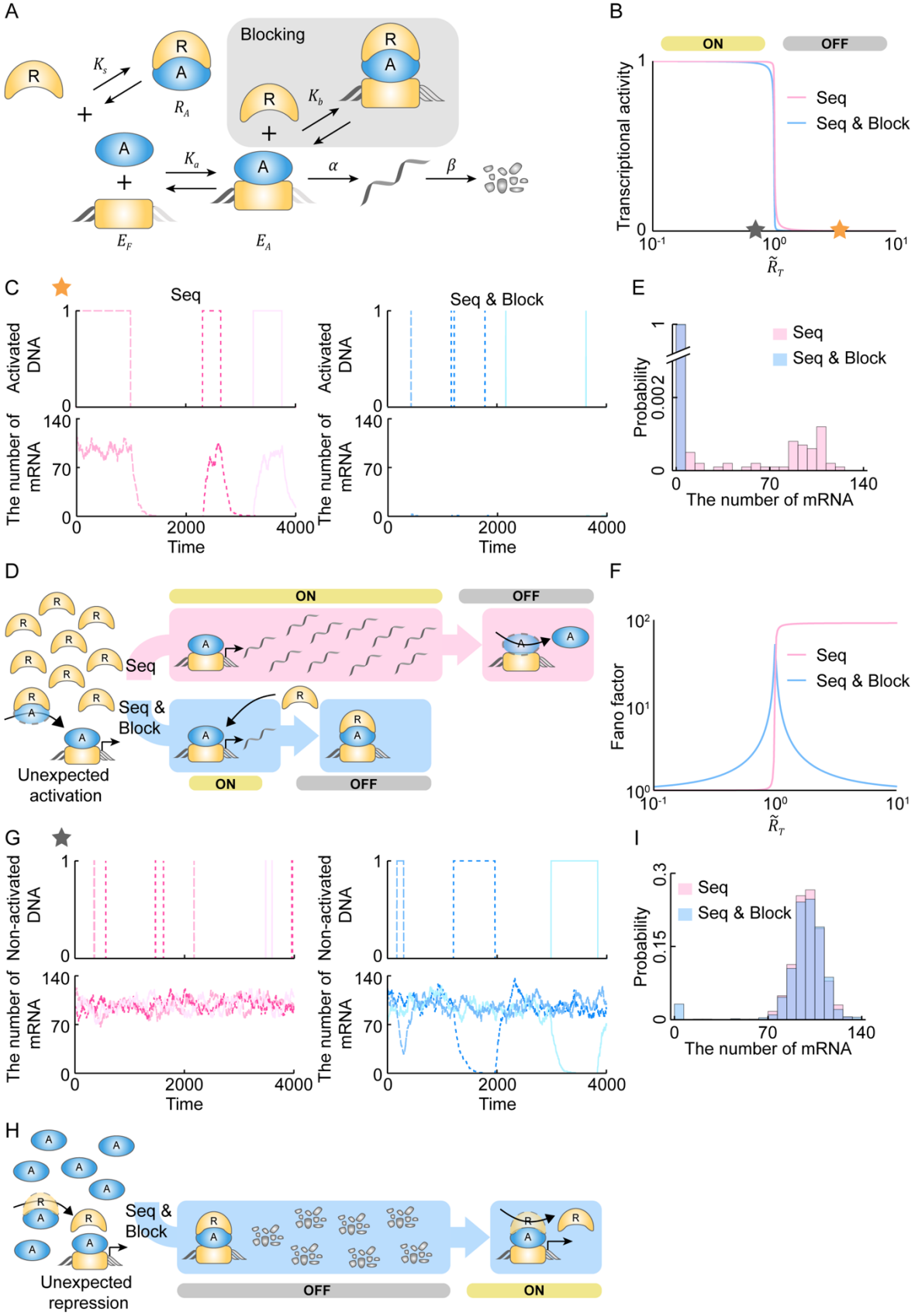

Figure 3. Transcriptional ultrasensitive switch based on the combination of sequestration and blocking is sensitive to noise during TAP due to undesired transcriptional repression. (A) The

blocking is added to the sole sequestration model. The repressor (R) binds to the DNA-bound-activator (E_A) with a dissociation constant of K_b to block the transcription (i.e., blocking; gray box). (B) The combination of the sequestration and blocking (blue line) generates an ultrasensitive switch similar to the sole sequestration (red line). (C) However, unlike the sole sequestration, the combination of the sequestration and blocking rapidly restores the undesired activation of DNA during TRP to the repressed state. (D) When unexpected binding of activator to DNA occurs during TRP, repressor rapidly inhibits the activator in the presence of blocking (blue arrow), but not in its absence (red arrow). (E) As a result, the stationary distribution of mRNA molecules is concentrated around zero (blue bars) without bimodality observed in the sole sequestration (red bars). (F) Thus, the noise level dramatically reduces during TRP in the presence of blocking. However, the addition of blocking to the sole sequestration increases the noise level during the TAP. (G) Such high transcriptional noise is due to undesired repression persists for a long-time even during TAP when blocking is added. Here, the timeseries of non-activated DNA (i.e., free or repressed DNA) and mRNA are simulated at $\widetilde{R_T} = 10^{-0.1}$ (gray star in (B)). (H) When noise-induced binding of R to DNA-bound-activator occurs (i.e, blocking occurs), due to their tight binding, the undesired repression during TAP persists for a long time. This leads to the sharp decrease mRNA near to zero. (I) As a result, the stationary distribution of mRNA molecules shows an additional peak around zero, leading to bimodality with blocking (blue bars) unlike sole sequestration (red bars).

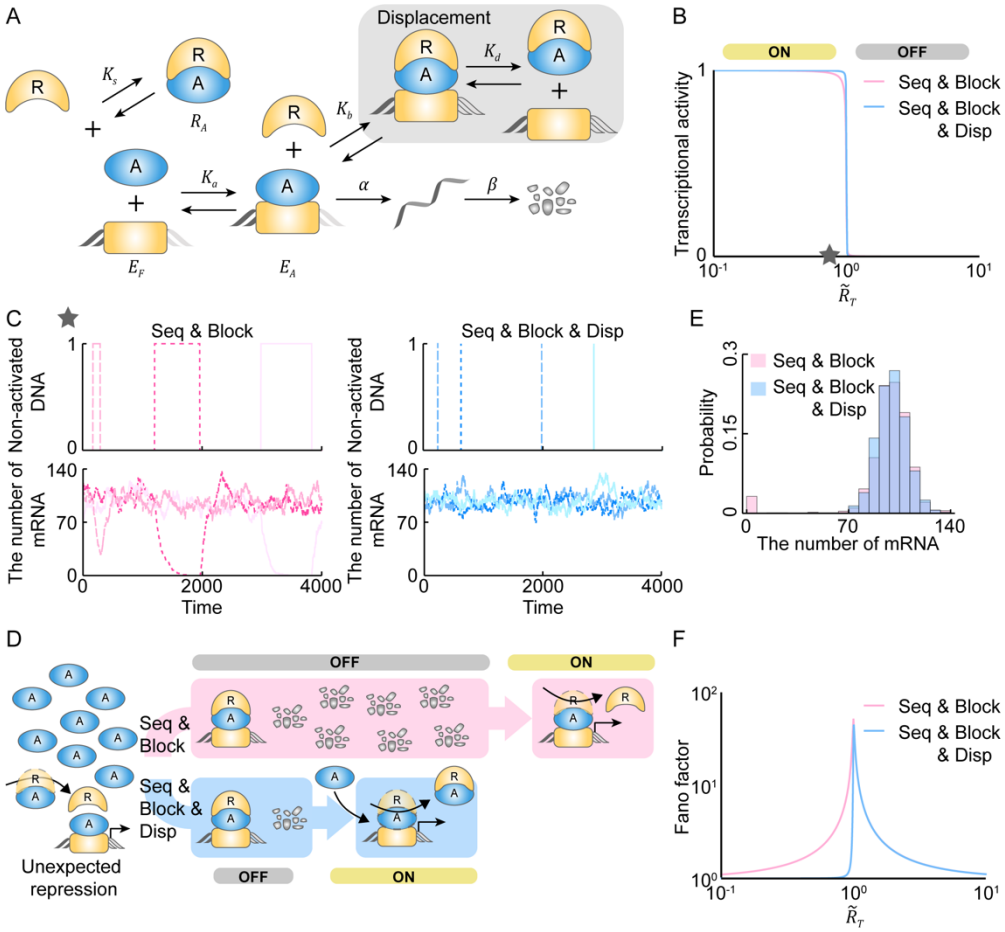

Figure 4. Transcriptional ultrasensitive switch based on the combination of sequestration, blocking, and displacement is robust to noise during both TAP and TRP. (A) The displacement is added to the combination of the blocking and sequestration model in Fig. 3(A). The repressor-activator complex (R_A) dissociates from DNA (E_R) with a dissociation constant of K_d to inhibit the transcription (i.e., displacement; gray box). (B) The combination of the sequestration, blocking and displacement (blue line) generates an ultrasensitive switch similar to the sequestration and blocking (red line). (C) With the addition of displacement, the undesired repression of DNA during TAP is rapidly restored to the activated state. (D) When unexpected repression occurs during TAP, repressor-activator complex dissociates from DNA for free activator to promote transcription immediately in the presence of displacement (blue arrow), but not in its absence (red arrow). (E) As a result, an additional peak around zero, observed in the combination of the sequestration and blocking (red bars), is removed from the stationary distribution of mRNA (blue bars). (F) Thus, the addition of displacement leads to the reduction in the noise level during TAP.